

Video Article

Controlling the Size, Shape and Stability of Supramolecular Polymers in Water

Pol Besenius¹, Isja de Feijter², Nico A.J.M. Sommerdijk³, Paul H.H. Bomans³, Anja R. A. Palmans²¹Organic Chemistry Institute and CeNTech, Westfälische Wilhelms-Universität Münster²Laboratory of Macromolecular and Organic Chemistry, Institute for Complex Molecular Systems, Eindhoven University of Technology³Laboratory of Materials and Interface Chemistry and Soft Matter Research Unit, Department of Chemical Engineering and Chemistry, Eindhoven University of TechnologyCorrespondence to: Anja R. A. Palmans at A.Palmans@tue.nlURL: <https://www.jove.com/video/3975>DOI: [doi:10.3791/3975](https://doi.org/10.3791/3975)

Keywords: Chemical Engineering, Issue 66, Chemistry, Physics, Self-assembly, cryogenic transmission electron microscopy, circular dichroism, controlled architecture, discotic amphiphile

Date Published: 8/2/2012

Citation: Besenius, P., de Feijter, I., Sommerdijk, N.A., Bomans, P.H., Palmans, A.R. Controlling the Size, Shape and Stability of Supramolecular Polymers in Water. *J. Vis. Exp.* (66), e3975, doi:10.3791/3975 (2012).

Abstract

For aqueous based supramolecular polymers, the simultaneous control over shape, size and stability is very difficult¹. At the same time, the ability to do so is highly important in view of a number of applications in functional soft matter including electronics, biomedical engineering, and sensors. In the past, successful strategies to control the size and shape of supramolecular polymers typically focused on the use of templates^{2,3}, end cappers⁴ or selective solvent techniques⁵.

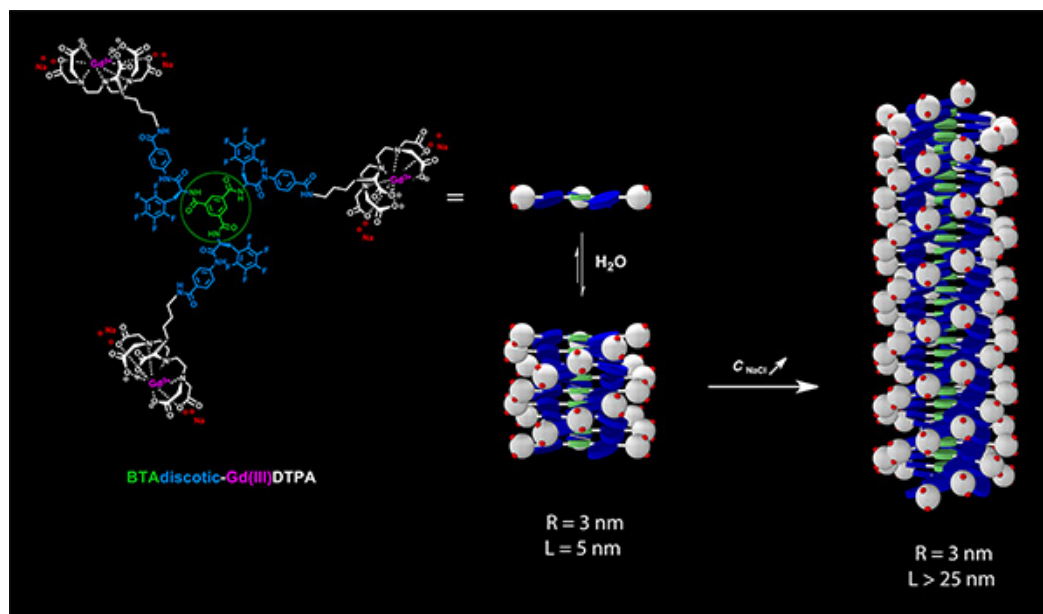
Here we disclose a strategy based on self-assembling discotic amphiphiles that leads to the control over stack length and shape of ordered, chiral columnar aggregates. By balancing electrostatic repulsive interactions on the hydrophilic rim and attractive non-covalent forces within the hydrophobic core of the polymerizing building block, we manage to create small and discrete spherical objects^{6,7}. Increasing the salt concentration to screen the charges induces a sphere-to-rod transition. Intriguingly, this transition is expressed in an increase of cooperativity in the temperature-dependent self-assembly mechanism, and more stable aggregates are obtained.

For our study we select a benzene-1,3,5-tricarboxamide (BTA) core connected to a hydrophilic metal chelate via a hydrophobic, fluorinated L-phenylalanine based spacer (**Scheme 1**). The metal chelate selected is a Gd(III)-DTPA complex that contains two overall remaining charges per complex and necessarily two counter ions. The one-dimensional growth of the aggregate is directed by π - π stacking and intermolecular hydrogen bonding. However, the electrostatic, repulsive forces that arise from the charges on the Gd(III)-DTPA complex start limiting the one-dimensional growth of the BTA-based discotic once a certain size is reached. At millimolar concentrations the formed aggregate has a spherical shape and a diameter of around 5 nm as inferred from ¹H-NMR spectroscopy, small angle X-ray scattering, and cryogenic transmission electron microscopy (cryo-TEM). The strength of the electrostatic repulsive interactions between molecules can be reduced by increasing the salt concentration of the buffered solutions. This screening of the charges induces a transition from spherical aggregates into elongated rods with a length > 25 nm. Cryo-TEM allows to visualise the changes in shape and size. In addition, CD spectroscopy permits to derive the mechanistic details of the self-assembly processes before and after the addition of salt. Importantly, the cooperativity -a key feature that dictates the physical properties of the produced supramolecular polymers- increases dramatically upon screening the electrostatic interactions. This increase in cooperativity results in a significant increase in the molecular weight of the formed supramolecular polymers in water.

Video Link

The video component of this article can be found at <https://www.jove.com/video/3975/>

Protocol



Scheme 1. Self-assembly of BTA-based discotics in citrate buffer into spherical aggregates showing diameters of about 5 nm, at millimolar concentrations of building block. Increasing the ionic strength by the addition of NaCl results in the formation of elongated rods with a diameter of around 3 nm and length > 25 nm. [Click here to view larger figure.](#)

1. Preparing a BTA-Gd(III)DTPA Solutions for CD Spectroscopy and Measurement of Temperature-dependent CD Spectra as a Function of NaCl Concentration

1. Prepare a 100 mM citrate buffer (pH 6.0).
2. Prepare a 100 mM citrate buffer (pH 6.0) with 2 M NaCl.
3. Dissolve 0.254 mg of **BTA-Gd(III)DTPA** (MW = 3184 g·mol⁻¹) in 10 mL of 100 mM citrate buffer, target concentration 8·10⁻³ mM of **BTA-Gd(III)DTPA**.
4. Sonicate the solution for 5 minutes.
5. Fill a 1 cm UV cuvet with the solution and measure a CD spectrum from 230 to 350 nm and a CD cooling curve at the highest intensity CD band (e.g. λ = 269 nm) from 363 - 283 K at a rate of 1 K min⁻¹.
6. Add the same volume of 2 M NaCl buffered solution to the citrate buffered solution of **BTA-Gd(III)DTPA** in order to increase the ionic strength to 1 M NaCl, diluting the discotics to half the concentration, target concentration 4·10⁻³ mM of **BTA-Gd(III)DTPA**.
7. Vortex the solution with increased ionic strength for 5 minutes.
8. Remeasure a CD spectrum from 230 to 350 nm and a CD cooling curve at the highest intensity CD band from 363 - 283 K at a rate of 1 K min⁻¹.

2. Fitting the T-dependent CD Data to a Model for T-dependent Self-assembly

1. The raw CD data were exported into Origin 8.5 and normalized. This was achieved by defining the CD effect at the highest measured temperature as equal to 0, and the CD effect at lowest measured temperature as equal to 1. Since the magnitude of the CD-effect is proportional to the degree of aggregation⁸, the normalized CD-curves are proportional to the degree of aggregation.
2. The normalized data were fitted using the nonlinear curve fit option in OriginPro 8.5 using a T-dependent self-assembly model derived by van der Schoot^{8,9}. In this model, a nucleation and an elongation regime are distinguished. First the degree of aggregation in the elongation regime ($T < T_e$) was fitted, using the following equation:

$$\phi_n = \phi_{SAT} \left[1 - \exp\left(\frac{-h_e}{RT_e^2} (T - T_e)\right) \right]$$

Above equation contains (next to the variable temperature, T , and the degree of aggregation, ϕ_n) three parameters; *i.e.* the enthalpy of elongation h_e , the elongation temperature T_e (the temperature at which the self-assembly starts) and the parameter ϕ_{SAT} , which is introduced to ensure that ϕ_n/ϕ_{SAT} does not exceed unity, which follows from the constraint that the degree of aggregation cannot exceed unity.

Fitting renders the enthalpy of elongation h_e (J/mol) and the elongation temperature T_e (K) that characterize the self-assembly of the molecules for a given concentration. When fitting, one restraint should be obeyed which is that only the degree of aggregation at temperatures below T_e should be fitted, since equation 2.1 is only valid in the elongation regime.

Next, the experimentally found degree of aggregation in the nucleation regime can be fitted, using the following equation:

$$\phi_n = \phi_{SAT} \left[\sqrt[3]{K_a} \exp \left[\left(\frac{2}{3 \cdot \sqrt[3]{K_a}} - 1 \right) \frac{h_e}{RT_e^2} (T - T_e) \right] \right]$$

Above equation contains (next to the variables T and ϕ_n) four parameters of which already three were determined with equation 2.1; *i.e.* the enthalpy of elongation h_e , the elongation temperature T_e and the parameter ϕ_{SAT} . The only unknown parameter is the K_a value -describing the cooperativity of the nucleation phase- which is found by fitting the experimentally found degree of aggregation for temperatures above T_e .

3. Preparing BTA-Gd(III)DTPA Solutions for Transmission Electron Microscopy and Visualization of Supramolecular Polymers via Cryogenic TEM

1. Prepare two buffers: a 100 mM citrate buffer (pH 6.0) and a 100 mM citrate buffer (pH 6.0) with 5 M NaCl.
2. Dissolve 0.318 mg of **BTA-Gd(III)DTPA** (MW = 3184 g·mol⁻¹) in 0.1 mL of each of the prepared buffers, target concentration 1 mM of **BTA-Gd(III)DTPA**.
3. The sample vitrification for cryogenic TEM is carried out using an automated vitrification robot (FEI Vitrobot Mark III). CryoTEM grids (R2/2 Quantifoil Jena grids from Quantifoil Micro Tools GmbH) are surface plasma treated prior to the vitrification procedure using a Cressington 208 carbon coater operating at 5 mA for 40 s. The aqueous solution is then applied on the grid during vitrification on an automated FEI Vitrobot. This involves the application of the sample on the grid, blotting of excess liquid to create a thin film of the aqueous solution on the grid and subsequent vitrification by dipping the grid very quickly in liquid ethane. After vitrification the sample is kept in liquid nitrogen and transferred manually on the autoloader cassette, also cooled with liquid nitrogen. The cassette is then inserted into the autoloader of the TEM. All this is done manually.
4. The cryoTEM experiments are performed on the TU/e cryoTITAN (FEI), (www.cryotem.nl). The TU/e cryoTITAN is equipped with a field emission gun (FEG) operating at 300 kV. Images were recorded using a 2k x 2k Gatan CCD camera equipped with a post column Gatan Energy Filter (GIF).

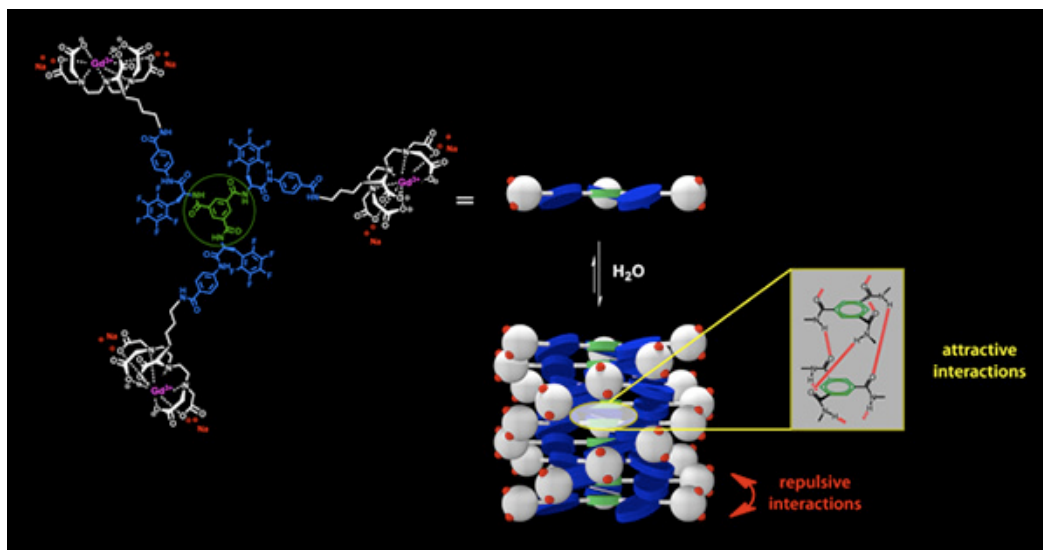
4. ¹H-DOSY NMR Measurements of Spherical Self-assembled BTA-Gd(III)DTPA at Low Ionic Strength

1. Prepare a 50 mM *d*₆-succinate buffer in D₂O ('pH 6.0'); the buffer is prepared by dissolving *d*₆-succinic acid in D₂O, followed by adjusting the pH to 6.0 using 1 M ND₄OD in D₂O. The final concentration of 50 mM succinate was adjusted with additional D₂O.
2. Since Gd(III) is highly paramagnetic and ¹H signals would thereby be broadened significantly, Gd(III) was substituted for Y(III).
3. Dissolve 2.98 mg of **BTA-Y(III)DTPA** (MW = 2979 g·mol⁻¹) in 1 mL of a 50 mM *d*₆-succinate buffer in D₂O ('pH 6.0'), target concentration 1 mM **BTA-Y(III)DTPA**.
4. The ¹H-DOSY NMR measurements are carried out on a Varian Unity Inova 500 spectrometer equipped with a 5 mm ID-PFG probe from Varian. The DOSY experiments were carried out using the DOSY one-shot (Doneshot, Varian) pulse sequence. The 90 degree pulse and mixing times were adapted accordingly. Chemical shifts were referenced using the chemical shift of the 3-(trimethylsilyl)propionic-2,2,3,3-[D₄] acid sodium salt (TMSP).
5. The self-diffusion of HDO was used to calibrate the measurements; it is known from literature that the self-diffusion of HDO in D₂O at 298 K is 19.0 × 10⁻⁹ m²·s⁻¹. As a reference, the self-diffusion of HDO in D₂O was measured in a VARIAN 2 Hz D₂O standard sample and calibrated to its standard value. The model used to calculate the hydrodynamic radii R_H of the aggregates is the Stokes-Einstein relation for the diffusion of a spherical particle.

5. Representative Results

¹H-DOSY NMR and SAXS measurements on BTA-M(III)-DTPA: spherical objects in citrate buffer

The ionic character of the peripheral Gd(III) complexes introduces frustration in the one-dimensional growth of the discotic monomers whose core is designed to polymerize into elongated rod-like aggregates. The balance between attractive and repulsive interactions controls the size and the shape of the aggregates (**Scheme 2**).



Scheme 2.

A powerful technique to determine the size and the shape of particles in solution is synchrotron source small angle X-ray scattering (SAXS). BTA-Gd(III)-DTPA was dissolved in a citrate buffer solution and the SAXS profiles were recorded and fitted in the region $0.01 < q < 0.1 \text{ \AA}^{-1}$. A slope approaching zero in the low- q region ($q < 0.06 \text{ \AA}^{-1}$) indicates a lack of shape anisotropy in the aggregate, suggesting the presence of spherical objects (Figure 1). The data measured at different concentrations were fitted using a homogeneous monodisperse spherical form factor leading to a calculated radius, R , of 3.2 nm. The calculated geometric radius of monomeric discotic BTA-Gd(III)-DTPA is 3.0 nm, which suggests the presence of aggregates with an aspect ratio close to 1.

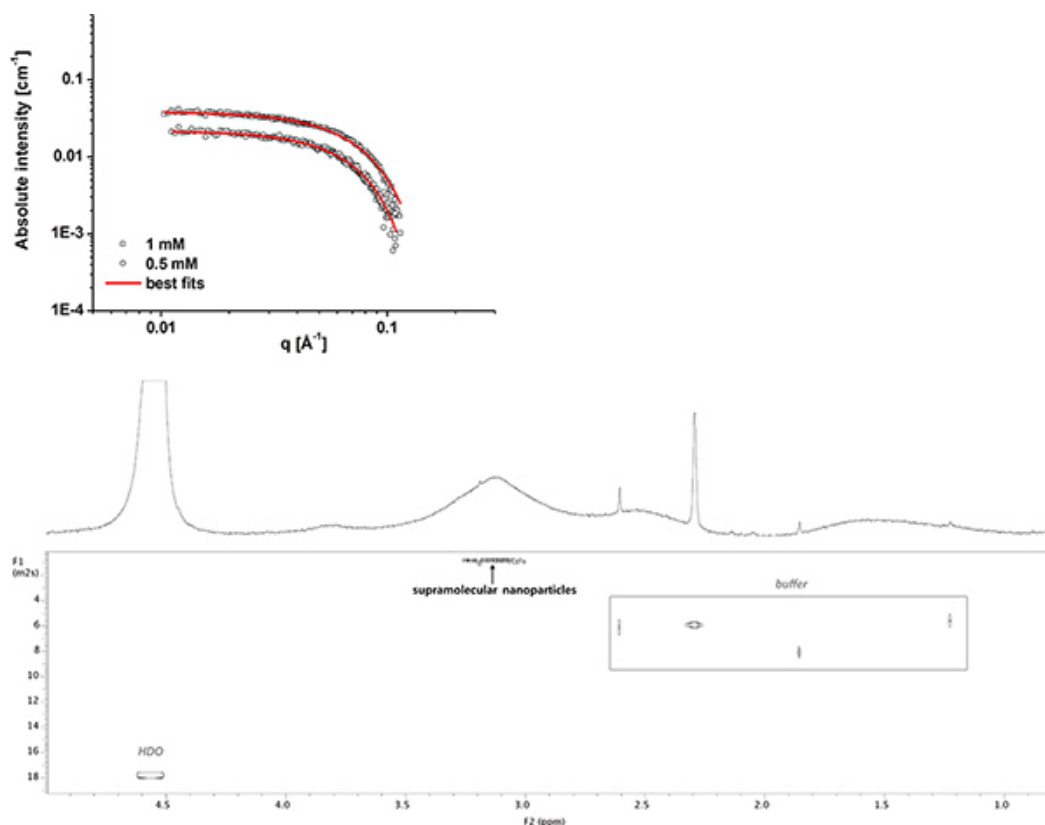


Figure 1. SAXS profiles for BTA-Gd(III)-DTPA in citrate buffer (100 mM, pH 6) at 0.5 and 1.0 mM (top). DOSY NMR of BTA-Y(III)-DTPA in 50 mM d_6 -succinate buffer at 1.0 mM (bottom). [Click here to view larger figure.](#)

In order to provide further evidence for the spherical shape and nanometer-size of the self-assembled objects, we performed ^1H diffusion-ordered NMR spectroscopy (^1H -DOSY NMR) (Figure 1). DOSY-NMR allows determination of the diffusion coefficients of aggregates, from which the hydrodynamic radius (R_H) can be calculated. Since Gd(III) is highly paramagnetic and ^1H signals would thereby be broadened significantly, we changed Gd(III) for diamagnetic Y(III). The diffusion coefficients of the aggregated diamagnetic discotic amphiphile in a deuterated succinate buffer (50 mM, pH 6, $c = 1 \text{ mM}$) was determined to be $0.69 \times 10^{-10} \text{ m}^2 \text{ s}^{-1}$. Via the Stokes-Einstein relation, we calculate a hydrodynamic radius

R_H of 2.9 nm for the discrete objects of spherical size (**Table 1**). This size is in excellent agreement with value obtained from SAXS data for BTA-Gd(III)-DTPA.

BTA-M(III)-DTPA [mM]	D_t^a [$10^{-10} \text{ m}^2\text{s}^{-1}$]	R_H^a [nm]	R^b [nm]
1	0.69	2.9	3.2

^a from DOSY; ^b from SAXS

Table 1. Results of SAXS and DOSY measurements for BTA-M(III)-DTPA.

Cryo-TEM on BTA-Gd(III)-DTPA: from spherical objects to elongated nanorods

Further evidence for successful control over one-dimensional stack length was obtained from cryo-TEM micrographs. Due to the vitrification of the aqueous solutions cryogenic TEM preserves the structural morphology of the self-assembled aggregates and avoids drying affects related to conventional TEM sample preparation. **Figure 2** (left) shows that BTA-Gd(III)-DTPA produces the expected spherical objects with diameters close to 6 nm at a 1 mM concentration, which confirms the results from SAXS and DOSY measurements. According to these findings, we have been able to obtain self-assembled discrete objects that can be considered the supramolecular equivalent of dendritic macromolecules¹⁰.

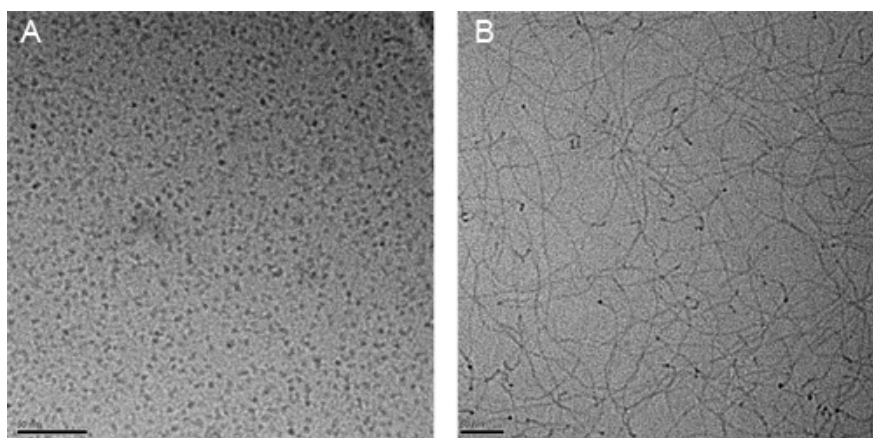


Figure 2. Cryo-TEM images for BTA-Gd(III)-DTPA (left) 1 mM vitrified at 298 K in citrate buffer (100 mM, pH 6), scale bar represents 50 nm; (right) 1 mM vitrified at 298 K in citrate buffer (100 mM, pH 6) and an overall NaCl concentration of 5 M, scale bar represents 50 nm.

So far we have only worked in buffered solutions of low ionic strength. However, if electrostatic repulsive forces of the peripheral charged M(III)-DTPA complexes on BTA-Gd(III)-DTPA are at the origin of the frustrated one-dimensional growth, we expected that increasing the ionic strength of the buffered environment, using an inert 1:1 salt with highly hydrated counterions, should reduce the electrostatic interactions and hence a different type of self-assembled object should be formed. In citrate buffer comprising 5 M NaCl this effect was indeed observed (**Figure 2, right**). The formation of high aspect ratio rod-like supramolecular polymers is clearly observed in cryo-TEM micrographs at high ionic strength. Electrostatic screening is the most likely explanation for this finding. The shape changes from a spherical aggregate of around 6 nm in diameter to elongated rods with a diameter of 6 nm and length of up to several hundred nanometers.

CD measurements of BTA-Gd(III)-DTPA: switching on cooperative self-assembly by increasing the ionic strength

Circular dichroism (CD) spectroscopy measures the difference in absorption between left-handed and right-handed circularly polarized light. When a helical object has a preferred helical sense, left- and right-handed circularly polarized light will be absorbed to different extents, hence giving rise to a CD-effect. Since the intermolecular hydrogen bonds formed between consecutive BTA-Gd(III)-DTPA within the aggregates, are lined up in a helical fashion and the stereogenic centre at the L-phenylalanine moiety favors one helical sense over the other, we expect a clear CD spectrum from BTA-Gd(III)-DTPA based aggregates^{11,12}. In addition, temperature-dependent CD spectroscopy is a powerful tool to assess the self-assembly mechanism of BTA-Gd(III)-DTPA polymerisation and allows to derive conclusions on the stability of the formed aggregates¹³.

As an example, the room temperature CD spectra of BTA-Gd(III)-DTPA (8×10^{-3} mM or 4×10^{-3} mM in a 100 mM citrate buffer) with increasing salt concentration (0 M NaCl to 1.0 M NaCl) are given in **Figure 3A**. Although a significantly lower concentration is applied for the CD measurements, the clear Cotton effect indicates the presence of intact aggregates, even at micromolar concentrations. The shape of the CD spectrum changes upon increasing the salt concentration, which is a good indication for reduced interactions at the periphery of the stacks and better packing of the discotics. In addition, the CD cooling curves of the same solutions (363 - 283 K, measured at $\lambda = 269$ or 278 nm) show distinct differences in shape (**Figure 3B**). The apparent T_e -the temperature at which aggregation starts- shifts to higher temperatures at higher salt concentration and an increasingly cooperative mechanism, characterized by a more abrupt increase in the CD-effect, becomes apparent. Whereas the cooling curve at 0 M NaCl is best described by an isodesmic self-assembly process, the cooling curve at 1.0 M NaCl is typical for a cooperative self-assembly process¹⁴. In the former case, all association constants are assumed to be equal while in the latter case self-assembly occurs in at least two distinct stages. In the first step, a "nucleus" needs to be formed which is energetically highly unfavorable. After cooling below a critical polymerization temperature, elongation and exponential growth into supramolecular polymers of high molecular weight follows. Quantifying the thermodynamic parameters of the self-assembly of BTA-Gd(III)-DTPA at 0 and 1 M NaCl using a cooperative model clearly reveals the decrease

in K_a , which is the dimensionless activation constant⁸. Lower values for K_a indicate a higher degree of cooperativity in the self-assembly process, which is expressed in the formation of highly elongated supramolecular polymers as observed in cryo-TEM.

BTA-Gd(III)-DTPA	C_{NaCl}	K_a
8×10^{-3} mM	0 M	$5 \cdot 10^{-2}$
4×10^{-3} mM	1 M	$1 \cdot 10^{-4}$

Table 2. Degree of cooperativity expressed by K_a in the temperature-dependent self-assembly of BTA-Gd(III)-DTPA as a function of the NaCl concentration (C_{NaCl}).

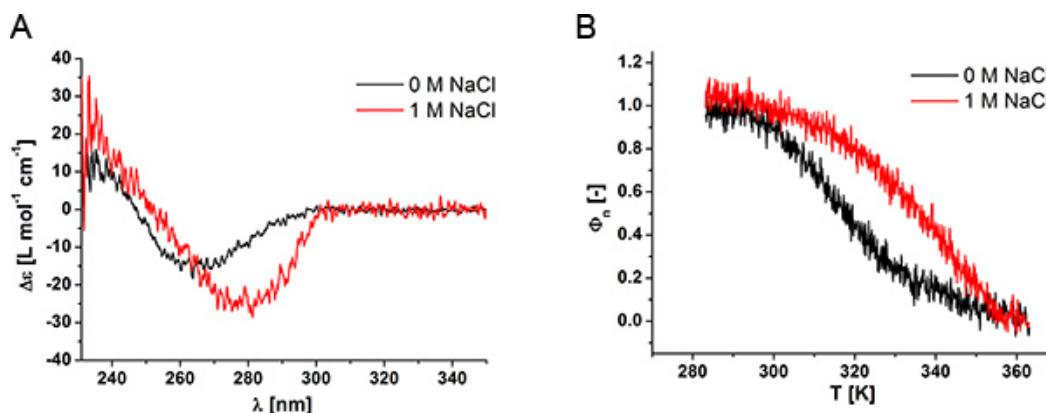


Figure 3. BTA-Gd(III)-DTPA in a 100 mM citrate buffer ($c = 8 \times 10^{-3}$ mM at low ionic strength and 4×10^{-3} mM at high ionic strength) A] CD spectra recorded at 293 K as a function of the ionic strength, $C_{\text{NaCl}} = 0$ M - 1.0 M, the molar ellipticity $\Delta\epsilon$ is calculated as follows: $\Delta\epsilon = \text{CD-effect}/(c \cdot l)$ in which c is the concentration of BTA in mol L^{-1} and l is the optical path length in cm; B] Corresponding CD cooling curves measured at $\lambda = 269$ nm for 0 M NaCl and 278 nm for 1 M NaCl solutions expressed as the degree of aggregation Φ_n as a function of the NaCl concentration $C_{\text{NaCl}} = 0$ M - 1.0 M, Φ_n is calculated by dividing the measured CD-effect by the maximal CD-effect.

Discussion

The self-assembling discotic amphiphiles discussed in this contribution containing the Gd(III)-DTPA complex are currently under investigation as novel magnetic resonance imaging (MRI) agents that combine high contrast with tunable excretion times.¹⁵ Hence, the details of their self-assembling behavior and their stability in different conditions are of critical importance. The combination of spectroscopic (CD and NMR), scattering (SAXS) and microscopy (cryo-TEM) techniques allows visualization of the formed structures and the quantification of their thermodynamic parameters. This combination of techniques is generally applicable for self-assembling molecules as long as a preferential helical sense in the studied system allows a difference in the absorption of left- and right-handed circularly polarized light.

Disclosures

No conflicts of interest declared.

Acknowledgements

The authors gratefully acknowledge Marko Nieuwenhuizen for assistance with the DOSY-NMR.

References

- Palmer, L.C. & Stupp, S.I. Molecular self-assembly into one-dimensional nanostructures. *Acc. Chem. Res.* **41**, 1674-1684 (2008).
- Janssen, P.G.A., Vandenbergh, J., van Dongen, J.L.J., Meijer, E.W., & Schenning, A.P.H.J. ssDNA templated self-assembly of chromophores. *J. Am. Chem. Soc.* **129**, 6078-6079 (2007).
- Bull, S.R., Palmer, L.C., Fry, N.J., Greenfield, M.A., Messmore, B.W., Meade, T.J., & Stupp, S.I. A templating approach for monodisperse self-assembled organic nanostructures. *J. Am. Chem. Soc.* **130**, 2742-2743 (2008).
- Lortie, F., Boileau, S., Bouteiller, L., Chassenieux, C., & Lauprêtre, F. Chain stopper-assisted characterization of supramolecular polymers. *Macromolecules.* **38**, 5283-5287 (2005).
- Wang, X., Guerin, G., Wang, H., Wang, Y., Manners, I., & Winnik, M.A. Cylindrical block copolymer micelles and co-micelles of controlled length and architecture. *Science.* **317**, 644-647 (2007).
- Besenius, P., Portale, G., Bomans, P.H.H., Janssen, H.M., & Palmans, A.R.A., Meijer, E.W. Controlling the growth and shape of chiral supramolecular polymers in water. *Proc. Natl. Acad. Sci. U.S.A.* **107**, 17888-17893 (2010).
- Besenius, P., van den Hout, K.P., Albers, H.M.H.G., de Greef, T.F.A., Olijve, L.L.C., Hermans, T.M., de Waal, B.F. M., Bomans, P.H.H., Sommerdijk, N.A.J.M., Portale, G., Palmans, A.R.A., van Genderen, M.H.P., Vekemans, J.A.J.M., & Meijer, E.W. Controlled supramolecular oligomerisation of C3-symmetrical molecules in water: the impact of hydrophobic shielding. *Chem. Eur. J.* **17**, 5193-5203 (2011).

8. Smulders, M.M.J., Schenning, A.P.H.J., & Meijer, E.W. Insights into the mechanisms of cooperative self-assembly: the sergeants-and-soldiers principle of chiral and achiral C₃-symmetrical discotic triamides. *J. Am. Chem. Soc.* **130**, 606-611 (2008).
9. Jonkheijm, P., van der Schoot, P., Schenning, A.P.H.J., & Meijer, E.W. Probing the solvent-assisted nucleation pathway in chemical self-assembly. *Science*. **313**, 80-83 (2006).
10. Bosman, A.W., Janssen H.M., & Meijer, E.W. About dendrimers: structure, physical properties, and applications. *Chem. Rev.* **99**, 1665-1688 (1999).
11. Veld, M.A.J., Haveman, D., Palmans, A.R.A., & Meijer, E.W. Sterically demanding benzene-1,3,5-tricarboxamides: tuning the mechanisms of supramolecular polymerization and chiral amplification. *Soft Matter*. **7**, 524-531 (2011).
12. Stals, P.J.M., Smulders, M.M.J., Martín-Rapún, R., Palmans, A.R.A., & Meijer, E.W. Asymmetrically substituted benzene-1,3,5-tricarboxamides: self-assembly and odd-even effects in the solid state and in dilute solution. *Chem. Eur. J.* **15**, 2071-2080 (2009).
13. De Greef, T.F.A., Smulders, M.M.J., Wolfs, M., Schenning, A.P.H.J., Sijbesma, R.P., & Meijer, E.W. Supramolecular polymerization. *Chem. Rev.* **109**, 5687-5754 (2009).
14. Smulders, M.M.J., Nieuwenhuizen, M.M.L., de Greef, T.F.A., van der Schoot, P., Schenning, A.P.H.J., & Meijer, E.W. How to distinguish isodesmic from cooperative supramolecular polymerization? *Chem. Eur. J.* **16**, 362-367 (2010).
15. Besenius, P., Heynens, J.L.M., Straathof, R., Nieuwenhuizen, M.M.L., Bomans, P.H.H., Terreno, E., Aime, S., Strijkers, G.J., Nicolay, K., & Meijer E.W. Paramagnetic self-assembled nanoparticles as supramolecular MRI contrast agents. *Contrast Media Mol. Imaging.*, In press, DOI: 10.1002/cmml.498 (2012).